Rheology and Microstructure of Functionalized Polymer-Modified Asphalt

J. M. Rojas,[1] N. A. Hernández,[1] O. Manero,[2] J. Revilla[1]

[1]*CID, Centro de Investigación y Desarrollo Tecnológico S.A. de C.V. (Grupo DESC) Av. de los Sauces No. 87 manzana 6, Parque Industrial Lerma. Lerma, 52000 México*
[2]*Instituto de Investigaciones en Materiales, Facultad de Química. UNAM A.P. 70-360. México, D.F., 04510 México*

Received 24 October 2007; accepted 3 June 2008
DOI 10.1002/app.28953
Published online 25 August 2009 in Wiley InterScience (www.interscience.wiley.com).

ABSTRACT: Viscoelastic and morphological properties of functionalized-polymer-modified asphalt, FPMA, have been described as function of number of epoxy groups presented in the functionalized polymer. At low temperatures, simple viscoelastic models can predict the elastic response of FPMA at short times and its viscous behavior at long times. The increase of epoxy groups yielded an increase on activation energy for viscous deformation of FPMA, and so, on its resistance to irreversible deformations under strain cycles. From ambient to higher temperatures, emulsion model can predict rheological properties of FPMA because they behave as viscoelastic emulsions. Modification of relaxation spectrum for FPMA due to the presence of a polymer network was not as strong as in normal PMA, thus, the rheological behavior of FPMA was found similar to systems having weak networks. However, the network became stronger as the number of epoxy groups was increased. This trend was verified by morphology of FPMA. Emulsion-like structure was observed for all FPMA but differentiating each other by the polymer particle size. It was also observed that increase on epoxy groups, polymer particle size in the FPMA decreased, and higher stability at 180°C of FPMA was observed. © 2009 Wiley Periodicals, Inc. J Appl Polym Sci 115: 15–25, 2010

Key words: polymer-modified asphalt; functionalized copolymer; rheological modeling

INTRODUCTION

The purpose of asphalt modification with polymer is to improve the resistance to high temperature permanent deformation and fatigue (reduction of creep), to increase low temperature flexibility (less brittleness), and to reduce temperature susceptibility, improving impact properties at intermediate temperatures.[1,2]

The formation of homogeneous PMA is a function of asphalt composition; chemical structure, molecular weight, and degree of branching of the polymer; content of polymer; and the thermo-mechanical history of the material. The morphology of a PMA made with a styrene-butadiene-styrene (SBS) block copolymer consists of polymer-rich regions made of polymer swollen and dispersed in an asphalt matrix when the polymer is added in small amounts to the asphalt (up to 6 wt %), then, this morphology is well-known as emulsion-like. Also, SBS block copolymers can form a network in the asphalt through the polystyrene domains providing physical crosslinks.[3]

A means to provide better polymer dispersion in the asphalt is by forming chemical links between polymer and asphalt and improving compatibility, for example, adding sulphur to crosslink the polymer[4] with asphalt or reacting *in-situ* functional groups presented in a functionalized polymer with asphalt, that is, epoxy groups, acrylic acid, or maleic anhydride.[5] The effect of mixing time and temperature on the resulting compatibility has been critically assessed.[6] According to the aspect and fineness of the emulsion-like structure, a PMA with domains of the order of two microns has acceptable compatibility, and those between 10 and 20 microns are slightly compatible.

Asphalts have rather simple thermorheological properties. Their modulus master-curve shows two distinct regions: a glassy plateau and a viscous asymptote.[7] The addition of polymer to asphalt produces important rheological effects:[8,9] (i) increases the complex shear modulus response at low and intermediate frequencies, and induces a large decrease in the slope of dynamic master-curves. At the upper extreme of frequency, PMA exhibits rheological behavior similar to that of straight asphalt, (ii) PMA shows larger dispersion in the relaxation process than straight asphalt, which leads to an extension of

Correspondence to: J. Revilla (javier.revilla@desc.com.mx).
Contract grant sponsor: The Centre for research and Development of DESC (CID).

the relaxation to longer periods of time, (iii) stress relaxation curves develop a rubbery plateau at high polymer contents (above 6 wt %), and a significant decrease in loss tangent values are observed over almost the entire range of frequencies which suggests the formation of a polymer elastic network in the asphalt, and (iv) although, increases both the storage and loss moduli, the unequal rate of increase between these two variables is an overall decrease in loss tangent values. Consequently, polymer imparts a high level of elasticity to the asphalt. As polymer concentration increases, it was observed that a rubbery plateau gradually forms, indicating some sort of network evolution. A distinct maximum in the relaxation spectrum is indicative of the presence of a network-like structure. Also, important changes in morphology occur. Increasing the content of large rubber particles in the PMA produces both deviation from Newtonian behavior and an increase in the viscous modulus.

The presence of a network in the PMA is critical for optimal performance at elevated temperatures. The formation of a network is determined by polymer concentration and type, and polymer-asphalt interactions. The addition of a functionalized polymer[9,10] to the asphalt (i) improves compatibility of the PMA and formation of a network-like structure at lower polymer concentrations can be achieved, (ii) changes the shear viscosity behavior from Newtonian to power-law (induced pseudoplasticity), and (iii) increases the plateau modulus.

In this work, epoxy-functionalized tapered styrene-butadiene copolymers are used to obtain the functionalized-polymer-modified asphalt (FPMA) with a pavement-degree asphalt. A systematic analysis on the degree of polymer modification by these epoxy resins on the viscoelastic properties of the FPMA is carried out. Dynamic mechanical analysis was performed at low temperatures, and small-amplitude oscillatory shear measurements were carried out at ambient and high temperatures. In addition, morphology observations are related to the resulting viscoelastic characterization of the FPMA. From these results, it is possible to assess the performance of the FPMA from modeling of linear and nonlinear viscoelastic properties.

EXPERIMENTAL PART

Epoxy-functionalized tapered block copolymers of styrene-butadiene rubber with different level of functionalization up to five epoxy groups per polymer chain were used as asphalt modifiers. A two-step process was used to produce the tapered styrene-butadiene copolymers. The first step comprised an anionic polymerization in solution of styrene and 1,3-butadiene monomers. A batch stirred tank reactor, BSTR, was used to produce the copolymer. An inert gas (nitrogen) was used to maintain free of poisons the system, and cyclohexane was used as a solvent to dissipate the heat of reaction. After reaching 60°C, a given amount of styrene, S, and butadiene, B, monomers were added to the BSTR to produce a polymer with a mass relationship of 25/75 (S/B). Anionic polymerization in solution was carried out by using a stequiometric amount of *n*-butyl lithium to yield the copolymer with a desired molecular weight (110,000 g/mol measured by GPC). Ten minutes after the reaction peak temperature, a stequiometric amount of BHT was added to the reactor to finish the copolymerization. The second step of the process was an epoxy functionalization of double bounds in the butadiene part of the copolymer. Functionalization was made by using acetic peracid according to the Ohtsuka's process.[11]

The glass transition temperatures of polybutadiene and polystyrene blocks are −85°C and 100°C, respectively. Neat asphalt (AC-20) from Salamanca-Mexico was mixed with the functionalized copolymers using a Euromix® 33/300P high-shear mixer at 180°C, 2000 RPM, for 100 min in an inert atmosphere to avoid degradation and crosslinking reactions in the materials.

Creep measurements were made using a DMA analyser TA-Instruments 2980 on a three-point bending clamp under 1000 Pa mean oscillating force. Rheometrical measurements were made in a TA-Instruments AR2000 rheometer using parallel plates of 25 mm diameter. Small-amplitude oscillatory frequency sweeps were made at 25°C with 0.1% strain, from 0.1–100 rad/s. The rutting factor of the samples was obtained by performing a temperature sweep at 2°C/min from 40°C to 100°C at a frequency of 10 s^{-1} and 0.5% strain.

Fluorescence measurements were carried out on an Olympus microscope using 330 and 480 nm filters. In the resulting micrographs, the asphalt-rich phase appears dark, whereas the polymer-rich phase appears bright.

RESULTS AND DISCUSSION

Low temperature studies. Creep behavior

Measurements of low-temperature viscoelastic properties include dynamic mechanical analyses made on different PMA systems.[12] These data are important to assess the tensile strength and flexibility of PMA at low temperatures. Dynamic mechanical analysis provides the variation of flexural creep stiffness with time, whose slope is used to describe creep behavior. Up to strains of 1%

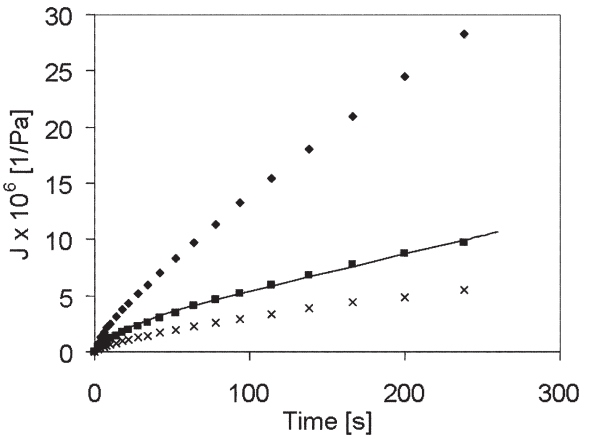

Figure 1 Shear compliance versus time for sample A at ◆ 0 °C, ■ -5 °C, — 5 °C (model), and × −10 °C. Predictions of the model shown in Fig. 4 are given as a continuous line.

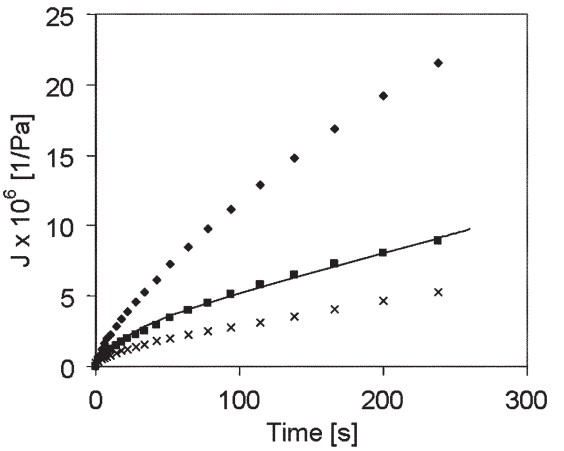

Figure 3 Shear compliance versus time for sample C. Same temperatures as in Fig. 1.

maintains the response in the linear viscoelastic region. The norm AASHTO MP-1 is based on the value of the mentioned slope and the value of the flexural creep stiffness at 60 s. At low temperatures, a good correlation was found between the rate of change of the flexural stiffness modulus with time and the fracture temperature for different PMA.[13] The creep stiffness has also been correlated to the loss tangent successfully.[14] Also, low temperature measurements are related to PMA resistance to low-temperature thermal cracking and fracture. Creep measurements give information on the degree of deformation of the FPMA as a function of time under constant stress. Results of the retardation curves (i.e. strain vs. time) for the three FPMA made with the styrene-butadiene copolymers containing various levels of reactive groups (two, three, and five epoxy groups/polymer chain, labeled A, B, and C) at a fixed polymer concentration (3.5 wt %) are shown in Figures. 1–3. Each figure contains data taken at three temperatures (0, −5, and −10°C). Under constant stress (0.001 N/mm^2 = 1000 Pa) the deformation of the samples decreases at lower temperatures, as expected. However, this decrease is not the same for each PMA, because the epoxy-group content modifies the polymer-asphalt interactions. To rationalize the experimental data, modeling of the creep curves for each sample at the three temperatures is attempted. It turns out that simple linear viscoelastic mechanical models, such as the Maxwell or Voigt models, are able to predict the retardation curves for each sample. In this case, the Maxwell-Voigt series combination, represented in Figure 4, can be applied to the creep data.

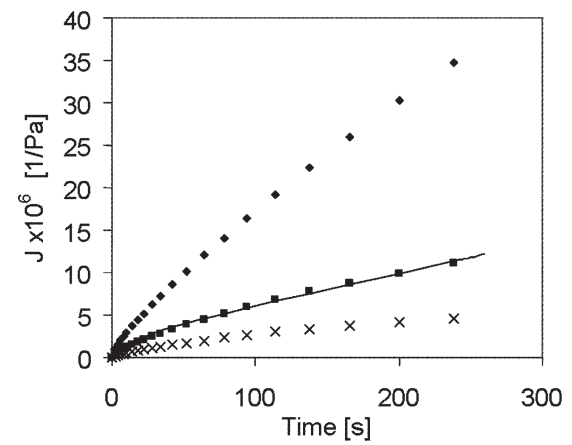

Figure 2 Shear compliance versus time for sample B. Same temperatures as in Fig. 1.

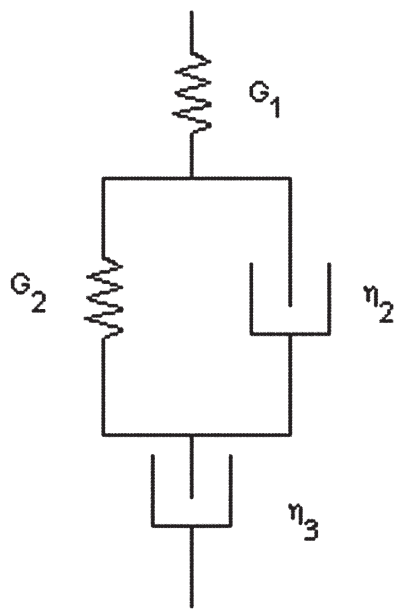

Figure 4 Maxwell-Voigt models in series.

TABLE I
Parameters of Maxwell–Voigt Model, *m*, and *S* of the FPMA

T (°C)	PMA	$G_1 \times 10^5$ (Pa)	$G_2 \times 10^5$ (Pa)	$\eta_2 \times 10^5$ (Pa)	$\eta_3 \times 10^5$ (Pa)	*m*	*S* at 60 s (MPa)
0	A	1.27	0.42	6.05	9.38	0.75	10.52
	B	1.06	0.32	8.42	7.65	0.76	8.60
	C	1.39	0.30	6.55	13.28	0.71	12.38
−5	A	2.33	0.59	13.69	30.40	0.66	25.85
	B	2.42	0.52	12.87	26.39	0.69	23.31
	C	2.31	0.51	13.18	35.46	0.63	26.50
−10	A	4.35	1.02	26.70	54.05	0.68	46.19
	B	5.03	0.99	29.95	67.11	0.67	53.00
	C	3.85	1.06	24.10	58.14	0.63	46.93

The retardation curve, that is, strain versus time under constant shear stress, for the model depicted in Figure 4 can be given by the following expression:

$$J(t) = \frac{1}{G_1} + \frac{1}{G_2}\left(1 - e^{\frac{t}{\lambda}}\right) + \frac{1}{\eta_3}t \quad (1)$$

Where $J(t)$ is the time-dependent shear compliance, G_1 and G_2 are the storage moduli, η_3 is the viscosity at long times, and λ is the retardation time. This characteristic time is given by:

$$\lambda = \frac{\eta_2}{G_2} \quad (2)$$

Equations (1) and (2) reproduce the experimental data adequately, as indicated by the bold black lines in Figures 1–3. The values of the four constants of the model are shown in Table I for each FPMA sample at the three temperatures of the experiments.

The norm AASHTO MP-1 indicates the range of recommended creep behavior for PMA according to the value of the slope *m* of the log–log plot of strain versus time (minimum = 0.3) and also to the value of the stiffness at 60 s (maximum = 300 MPa). In Figure 5, we show this plot for sample B (three epoxy groups grafted into the SB chain) at the three temperatures, together with the predictions of the model. In addition, in Table I the values of the slopes *m* and stiffness *S* at 60 s are also given for all the samples at the three temperatures. According to the values shown in Table I at −10°C, the sample B presents the largest stiffness value, whereas at 0°C, the slope is the largest with the lowest stiffness. Apparently, this sample is the most structured system.

From modeling of the creep curves, it is possible to show the variation of the relevant parameters of the model with temperature and with the degree of functionalization of the copolymer. In Figure 6(a,b) the variation of G_1 and η_3 is shown as the function of the epoxy content of copolymer, respectively. G_1 represents the instantaneous modulus, which is the inverse of the elastic compliance ($G_1 = 1/J_E$). η_3 is the viscosity in the linear region, and represents the viscous response of the system at long times. According to Figure 6(a), the instantaneous modulus G_1 is quite insensitive to the epoxy content, for the three temperatures, and only a slight decrease is observed as the functionalization level of the copolymer increases. This trend can be explained by the fact that asphalt modification with styrene-butadiene block copolymer is mainly done to modify intermediate and high temperatures, therefore, in the low temperature range; performance of PMA is more affected by asphalt. Moreover, epoxy groups in the polymer chain were used to react with asphalt during FPMA preparation; then stability between asphalt and polymer at high temperature was achieved; but low temperature mechanical resistance can remain similar to the normal PMA or they can show slightly increase on stiffness, *S*. Unfortunately, in our study, Samples A and C show similar behavior in both Stiffness *S* and *m*-value at all temperatures; Sample B shows an ambiguous behavior because at −10°C it is the sample with the highest stiffness *S* but at 0°C it has the lowest value, so

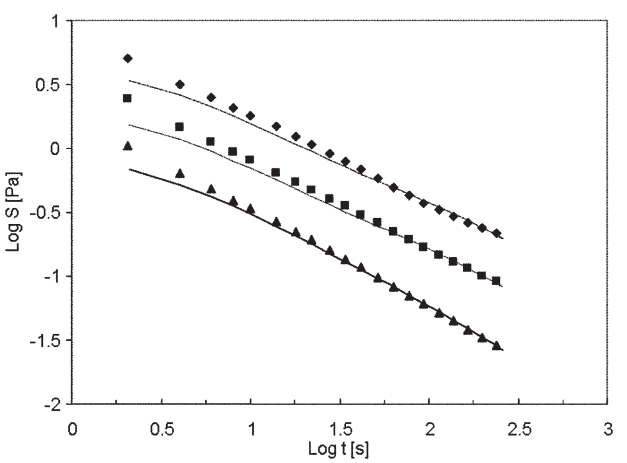

Figure 5 Stiffness versus time for sample B at ▲ 0 °C, — 0 °C (model), ■ −5 °C, --- −5 °C (model), ◆ −10 °C, and — - −10 °C (model). Predictions of the model shown in Fig. 4 are given.

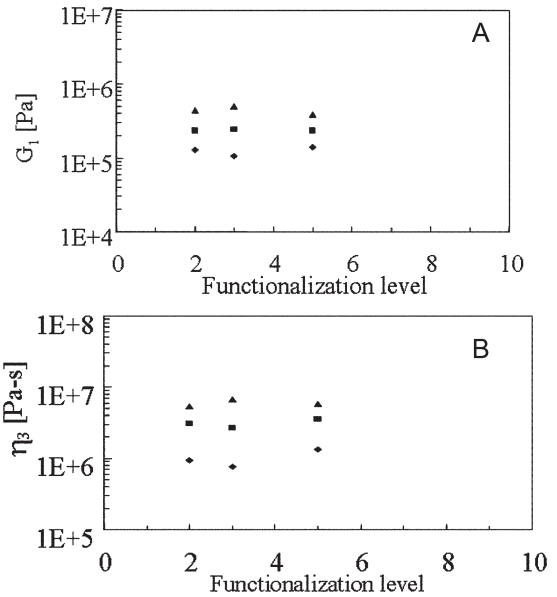

Figure 6 (A) Instantaneous modulus and (B) Long-time viscosity versus functionalization level of the copolymer at ◆ 0 °C, ■ −5 °C, and ▲ −10 °C.

stiffness S and the slope m did not show a clear behavior in function to the number of epoxy groups presented in the functionalized polymer. The viscosity of the FPMA, however, presents a change of behavior for temperatures higher than −10°C. At −5°C and 0°C, the viscosity of the FPMA increases as the functionalization level increases too. According to the reaction between epoxy groups and asphalt during FPMA preparation, a high number of epoxy groups can increase viscosity of the FPMA. Therefore, viscosity behavior at low temperature is in agreement to the functionalization level.

Figure 7(a,b) present the variation of the viscosity η_3 and elastic modulus G_1 of the FPMA with temperature, respectively. Although in a very short temperature range, the viscosity plotted with inverse temperature gives an estimation of the activation energy for the different FPMA [Fig. 7(a)]. The highest activation energy corresponds to sample B (130 KJ/mol) followed by the sample A (104 KJ/mol) and finally the lowest activation energy corresponds to sample C (88 KJ/mol). Then, Figure 7(a) relates the activation energy for viscous flow (or irreversible deformation under stress) with the degree of modification of the copolymer. It is apparent that sample B possesses the highest energy barrier to permanent deformation in the temperature range investigated. On the other hand, variation of the elastic modulus with temperature is a decreasing function, diminishing one decade each 15° approximately, as shown in Figure 7(b). Then, elastic modulus of the FPMA is quite insensitive to epoxy content at −5°C, and only slight differences are observed at −10°C and 0°C.

Ambient and high temperature studies. small-amplitude oscillatory shear flow

The rheology of PMA from 10 to 50°C is sensitive to straight asphalt characteristics, whereas above 50°C is dominated by the aggregate. High temperature viscosity related to the processing of asphalt and coating of aggregate is controlled by the rubber properties. At ambient temperatures, the viscous modulus, G'', is used to determine the degree of viscous component that is available to dissipate energy that would normally go towards crack propagation. This gives an indication of the resistance to load-associated fatigue crack propagation.[15] The basis of this relationship is the correlation of the dissipated energy, which is directly proportional to the loss modulus, with fatigue resistance. Because G'' is a measure of the viscous flow within a viscoelastic fluid, this parameter is related also to permanent deformation at ambient and higher temperatures, and gives indication of the resistance to load-associated fatigue crack propagation. In addition, the inverse of the shear loss compliance $(J'')^{-1} \cong G^*/\sin\delta \cong G^*$ is called rutting factor and measures the amount of nonrecoverable permanent deformation of asphalt binder and it can be related to the dynamic stiffness of the pavement when the loading frequency is in the range of vehicle traffic (1–16 Hz). These viscoelastic measurements can give valuable information

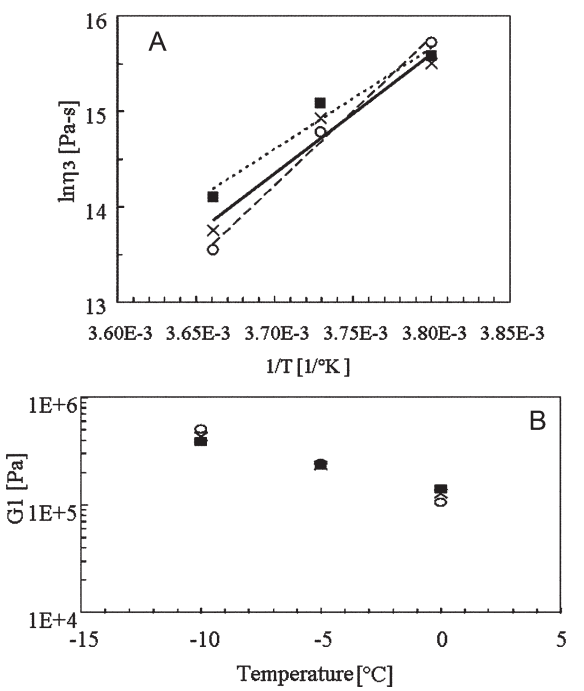

Figure 7 (A) Arrhenius plot of the viscosity at long times versus inverse temperature for the three FPMA. Activation energies are: A, 104.4 KJ/mol ×; B, 130 KJ/mol ○; C, 88 KJ/mol ■; (B) Semilog plot of the variation of the instantaneous modulus with temperature for the three FPMA (× A, ○ B, and ■ C).

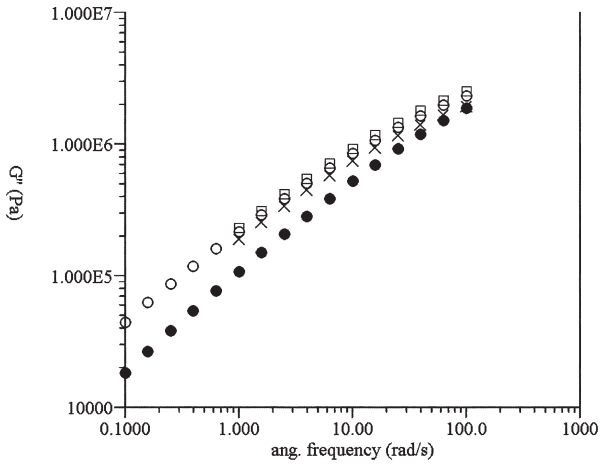

Figure 8 Variation of the loss modulus with angular frequency at ambient temperature for ● neat asphalt AC20 and the three FPMA (× A, ○ B, and □ C).

on the relationship between the viscoelastic properties of PMA and their performance in several applications.

In Figure 8, the loss modulus, G'', is plotted with frequency at 25°C. An increase in G'' is observed as the modified copolymer is added, although the rise in G'' is higher for sample C and it is lower for sample A. Then, It is clear that G'' increases as the functionalization level increases. However, the gap in G'' observed between the FPMA samples and neat asphalt diminishes when the frequency increases. The complex shear modulus is dominated by the loss modulus at low frequencies, and the addition of the modified copolymers induces a considerable decrease in the slope of the curves over this range of frequencies. The slope of G'' for this FPMA samples at low frequencies is 0.7, which is higher than that observed[16] in the flow of ordered block copolymers (0.5). Therefore, these systems do not form a rubbery plateau observed in SBS[2], nor an order–disorder transition is apparent. Rather, the functionalized groups generate associations that are likely to form a weak network.

The existence of the network could be seen by changes in loss tangent in function of frequency as shown in Figure 9(a). Increase in elasticity of PMA with the addition of epoxy-functionalized copolymer is reflected by the decrease in loss tangent over the whole range of frequencies, but it is observed that loss tangent of the FPMA is quite insensitive to the epoxy content.

The improvement in the asphalt viscoelastic properties brought about by the copolymer is clearly shown in Figure 9(b). The loss tangent of neat asphalt is a strong increasing function of temperature, leading to easy permanent deformation at high temperatures. The addition of functionalized copolymer keeps the value of the loss tangent lower enough within the 40–70°C to diminish permanent deformation of the FPMA. This level of elasticity at elevated temperatures is clearly due to a network structure, which is essential to prevent permanent deformation of FPMA. Also, it is well observed that above 70°C, sample A has the highest loss tangent value whereas sample C maintains the lowest loss tangent value. Therefore, elasticity of the FPMA increases as the functionalization level is increased, when the temperature is above 70°C.

One of the important tests for polymer-modified asphalts is the behavior of the inverse shear compliance with temperature, which estimates the dynamic stiffness of the pavement through measurements of permanent deformation subjected to loading cycles in the range of vehicle traffic (around 10 s^{-1}). Figure 10 exhibits the inverse shear compliance (rutting factor) as function of temperature at fixed frequency (10 s^{-1}) showing the action of the functionalized tapered styrene-butadiene copolymer on the behavior of the asphalt. Again, the dynamic stiffness is increased because of the presence of copolymer, especially at high temperatures, but sample C (highest epoxy content) has not the highest value of

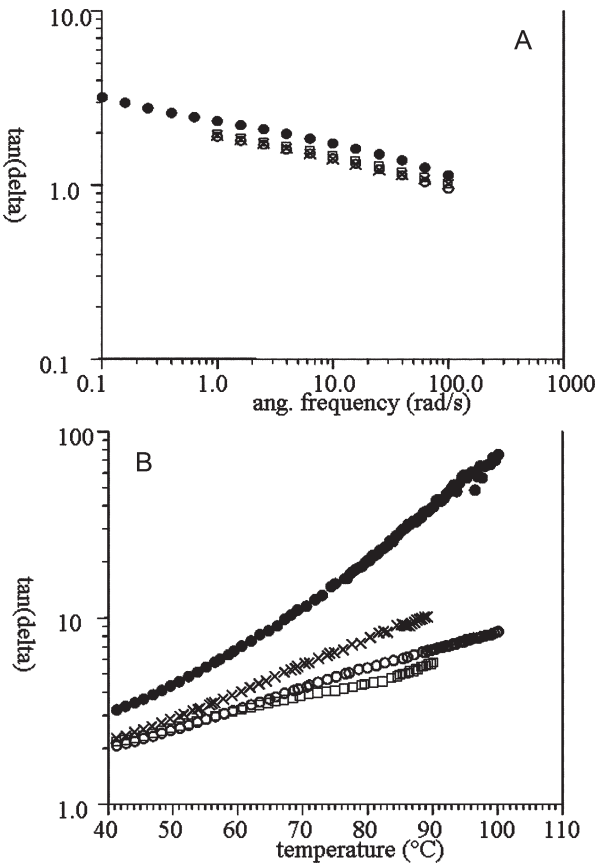

Figure 9 Variation of the loss tangent for ● neat asphalt AC20 and the three FPMA (× A, ○ B, and □ C) in function of (A) frequency at room temperature, and (B) temperature at fixed frequency.

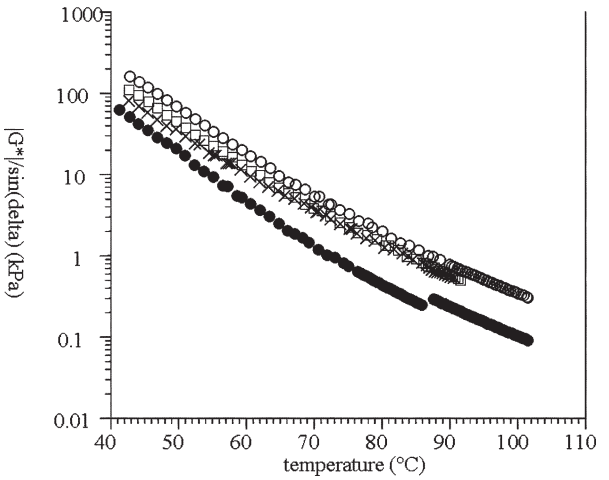

Figure 10 Variation of the inverse of the imaginary part of the complex compliance with temperature at fixed frequency for ● neat asphalt AC20 and the three FPMA (× A, ○ B, and □ C).

rutting factor as expected. Same data could be converted in a black diagram by plotting the phase angle versus log of the complex modulus, due to the fact that the time-temperature-superposition principle does not always hold for asphalts or their mixtures[17]. In Figure 11, a shallow minimum is observed at low modulus values (around 1000 Pa), more apparent in sample C (highest epoxy content). These minima in the phase angle have been attributed to a hard/soft relaxation[17]. As a consequence of this relaxation, the modulus of the FPMA in the region of the phase angle minimum is of the same order of magnitude as the modulus of the matrix and that of the dispersed phase. Hence, the location of the minimum may be associated to the modulus of the dispersed phase particles. So, black diagram shown in Figure 11 is the best way to elucidate polymer modification on asphalt than traditional plot of the rutting factor versus temperature presented in Figure 10.

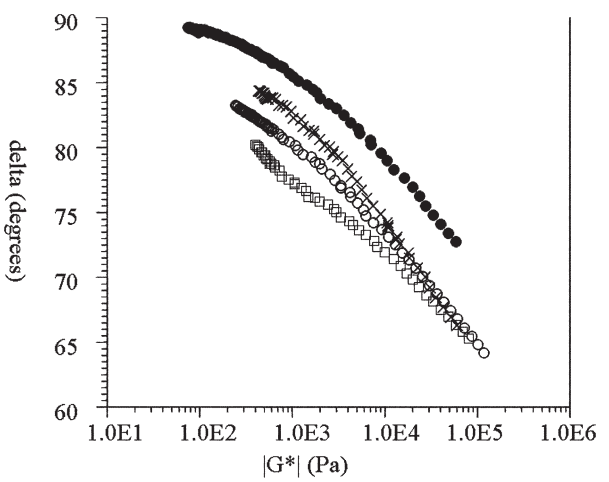

Figure 11 Black diagrams (phase angle versus complex modulus) of ● neat asphalt AC20 and the three FPMA (× A, ○ B, and □ C) at fixed frequency.

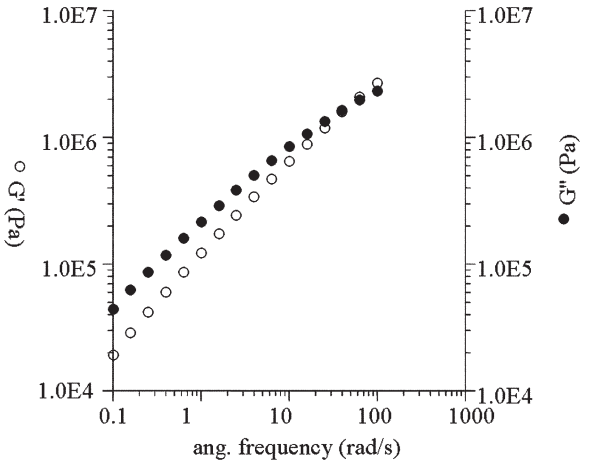

Figure 12 Elastic and loss modulus versus frequency at ambient temperature for sample B.

The crossing point of the elastic and loss modulus has been always referred to as the characteristic frequency, whose inverse is the main relaxation time of the system. Although the presence of copolymer induces a lower slope in the flow region that is a manifestation of additional longer relaxation times, the time associated to the crossing point signals the onset of elastic behavior for larger frequencies. In Figure 12, G' and G'' are plotted with frequency at fixed temperature (25°C) for sample B. Same plots (not shown) characterize the moduli behavior with frequency for the other FPMA and neat asphalt. Table II shows the variation of the characteristic time of the neat asphalt and the FPMA samples. This time is similar for neat asphalt and sample A (0.01 s) and increases slightly with epoxy content for samples B and C (0.013 s).

Prediction of linear viscoelastic properties at ambient and high temperatures was attempted using the Palierne emulsion model[18]. This approach considers that FPMA can be envisioned as an emulsion made of viscoelastic spherical inclusions in a viscoelastic matrix[16]. This model gives the complex modulus of the emulsion (G^*) as function of the complex modulus of the matrix, G_m^*, the complex modulus of the inclusions, G_i^*, the complex capillary number, Ca^*,

TABLE II
Frequency at Crossing Point, ω_c, and Mean Characteristic Relaxation Time, λ_c, of FPMA Samples

PMA	ω_c (rad/s)	λ_c (s)
AC-20	100	0.010
A	100	0.010
B	75	0.013
C	75	0.013

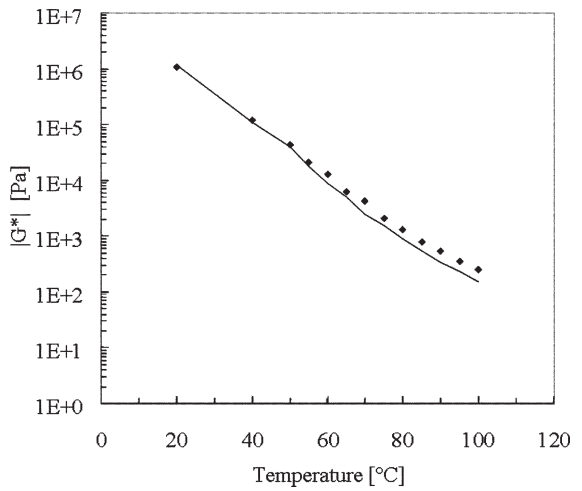

Figure 13 Variation of the complex modulus with temperature, showing the experimental data (sample B) and predictions of the emulsion model. Volume fraction = 0.3.

and the volume fraction of the dispersed phase, ϕ, according to the following expressions, which are valid for more than 10 vol % of the dispersed phase:

$$G^* = G_m^* \frac{1 + 1.5(E^*/D^*)\phi}{1 - (E^*/D^*)\phi} \quad (3)$$

$$E^* = 2(\lambda^* - 1)(19\lambda^* + 16) + 8(5\lambda^* + 2)/Ca^* \quad (4)$$

$$D^* = 2(\lambda^* + 3)(19\lambda^* + 16) + 40(\lambda^* + 1)/Ca^* \quad (5)$$

$$\lambda^* = \frac{G_i^*}{G_m^*} \quad (6)$$

$$Ca^* = G_m^* \left(\frac{a}{\gamma}\right) \quad (7)$$

Where γ is the interfacial tension, and a is the radius of the inclusion.

Evaluation of the dispersed phase properties was made on the neat epoxy-functionalized copolymers. Macrophase segregation in FPMA was not observed after 7 days storage in a vertical static tube at 180°C, and hence, the sample showed a high degree of stability. The size of the dispersed phase and the volume fraction were estimated from fluorescence micrographs, that is, Figure 16(a–c). For the different systems, the size of the inclusions was approximately about 10–15 microns and the volume fraction varied from 20 to 30%. As suggested by Lesueur et al.,[17] estimation of interfacial tension was made through a Cole-Cole representation of the complex viscosity at high temperature, where the droplet relaxation is the dominant mechanism. Application of Palierne model[18] led to values of the order of 10^{-5} N/m for the interfacial tension between the two phases. It turns out that the complex modulus of the matrix does not depend substantially on slight variations in the interfacial tension neither on the inclusions size.

The linear viscoelastic behavior of the FPMA was predicted using eqs. (3)–(7). As an example, the predicted values and the measured data for sample B are shown in Figure 13, where the complex modulus is plotted with temperature from 20 to 100°C. Predictions and data agree reasonable well in this temperature range for this sample.

According to Lesueur et al.,[19] micromechanical relaxations can occur due to competition between the viscous forces, which tend to deform the inclusions, and the forces restoring their spherical shapes, as the FPMA is heated from low to high temperatures. At relatively low temperatures, the system is composed of elastic particles and a rigid matrix. At high temperatures, the dispersed inclusions behave as viscous spheres with interfacial tension. In the first case, the restoring force is elastic and depends on the modulus of the inclusions, whereas in the second case the restoring force is the interfacial tension. As the temperature (at fixed frequency) of the FPMA increases from low to high values, the elastic dispersed particles lead first to a hard/soft relaxation[19] with a characteristic time τ_{hs} (if the matrix behaves as a Newtonian liquid) and, subsequently, the particles become viscous and lead to a droplet relaxation with a characteristic time[20] τ_d. These relaxations occur when the product of the characteristic time and frequency becomes one. The expressions of these times are:

$$\tau_{hs} = \frac{\eta_m}{G_i} \frac{2 + 3\phi}{2 - 2\phi} \quad (8)$$

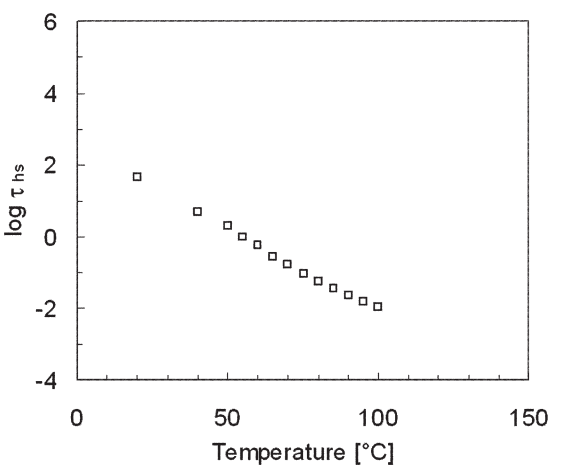

Figure 14 Semilog plots of the product of the frequency times the hard/soft relaxation time (τ_{hs}) versus temperature.

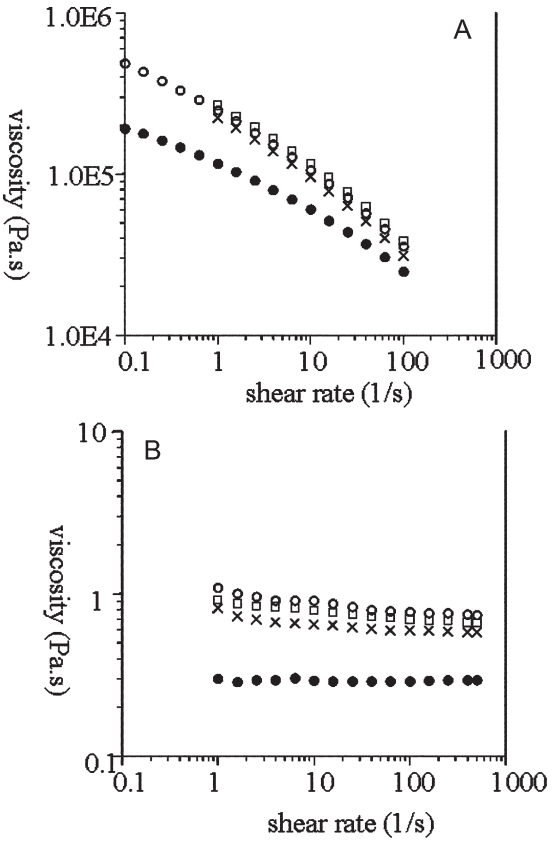

Figure 15 Shear viscosity as a function of shear rate for ● neat asphalt AC20 and the three FPMA (× A, ○ B, and □ C) at: (a) 25 °C, and (b) 160 °C.

$$\tau_d + \frac{1}{4}\frac{a\eta_m}{\gamma}\frac{(19\lambda+16)[2\lambda+3-2\phi(\lambda-1)]}{10(\lambda+1)-2\phi(5\lambda+2)} \qquad (9)$$

where η_m is the matrix viscosity. Figure 14 shows the variation of the product of frequency and these characteristic times with temperature, for sample B. It turns out that the hard/soft relaxation for this system is located at $\sim$ 57°C and the droplet relaxation time is very large and it is not observed in the experimental range of temperature. The value of the hard/soft relaxation time is close to that observed in PMA treated by Lesueur et al.,[17] that is, 52°C.

Nonlinear viscoelastic properties

The shear viscosity measured in a controlled stress mode is here studied as a function of shear rate for two temperatures (25 and 160°C). The effect of the polymer on the asphalt shear viscosity is to thicken the solution along a wide range of shear rates and to reduce the shear thinning behavior at high temperatures. In Figure 15(a), the shear viscosity at 25°C shows a pronounced thinning with a high-shear slope of −0.5 for all samples. Addition of epoxy-functionalized copolymers increases the viscosity of the FPMA several times, and the epoxy content has an effect on the rise of viscosity of FPMA. It is shown that an increase on epoxy content for functionalizing tapered styrene-butadiene copolymers yields an increase on viscosity at 25°C of the produced FPMA. When the temperature is risen to 160°C, the viscosity drops several decades but displays a drastic change in the rheological behavior, in this case the system becomes almost Newtonian, and the effect of copolymer is more pronounced. These results exhibit clearly the beneficial effect of epoxy-functionalized copolymer on the asphalt rheology, especially at high temperatures, where the formation of a network impedes the thinning of the PMA preventing irreversible deformations even when the amount of epoxy groups is not above 10%.

Morphology studies

Micrographs taken to the three FPMA samples are shown in Figure 16(a–c), corresponding to the three different epoxy levels investigated. The bright inclusions are the polymer-rich dispersed particles. The particle concentration is lower in Figure 16(a) and increases in Figure 16(b,c); it means that the increase of epoxy content into the tapered block styrene-butadiene copolymer should increase the particle concentration and change the inner morphology of the particle. All micrographs [Fig. 16(a–c)] show a well defined emulsion-like morphology for the whole FPMA, and a "salami" morphology into the dispersed polymer-rich particles. The main differences are size and number of dispersed particles observed in a similar area, and other difference found is the number of inclusions into the dispersed particles. Sample A show smallest dispersed particles with low number of inclusions in the asphalt rich matrix [Fig. 16(a)], whereas samples B and C show a very well defined salami morphology into the dispersed particles, and the size of dispersed particles are bigger than that of sample A. The morphology difference between sample B and C is the total number of dispersed particles observed in the same area. Then, a qualitative correlation between morphology and viscoelastic properties should be used because sample C has the highest elasticity (the lowest loss tangent versus temperature), and sample A has the lowest elasticity [Fig. 9(b)], and also sample C has the higher number of dispersed particles with well defined salami morphology.

In general, particle concentration is proportional to the magnitude of the viscoelastic quantities, that is, moduli, besides the widening of the relaxation spectrum brought about by the presence of copolymer.

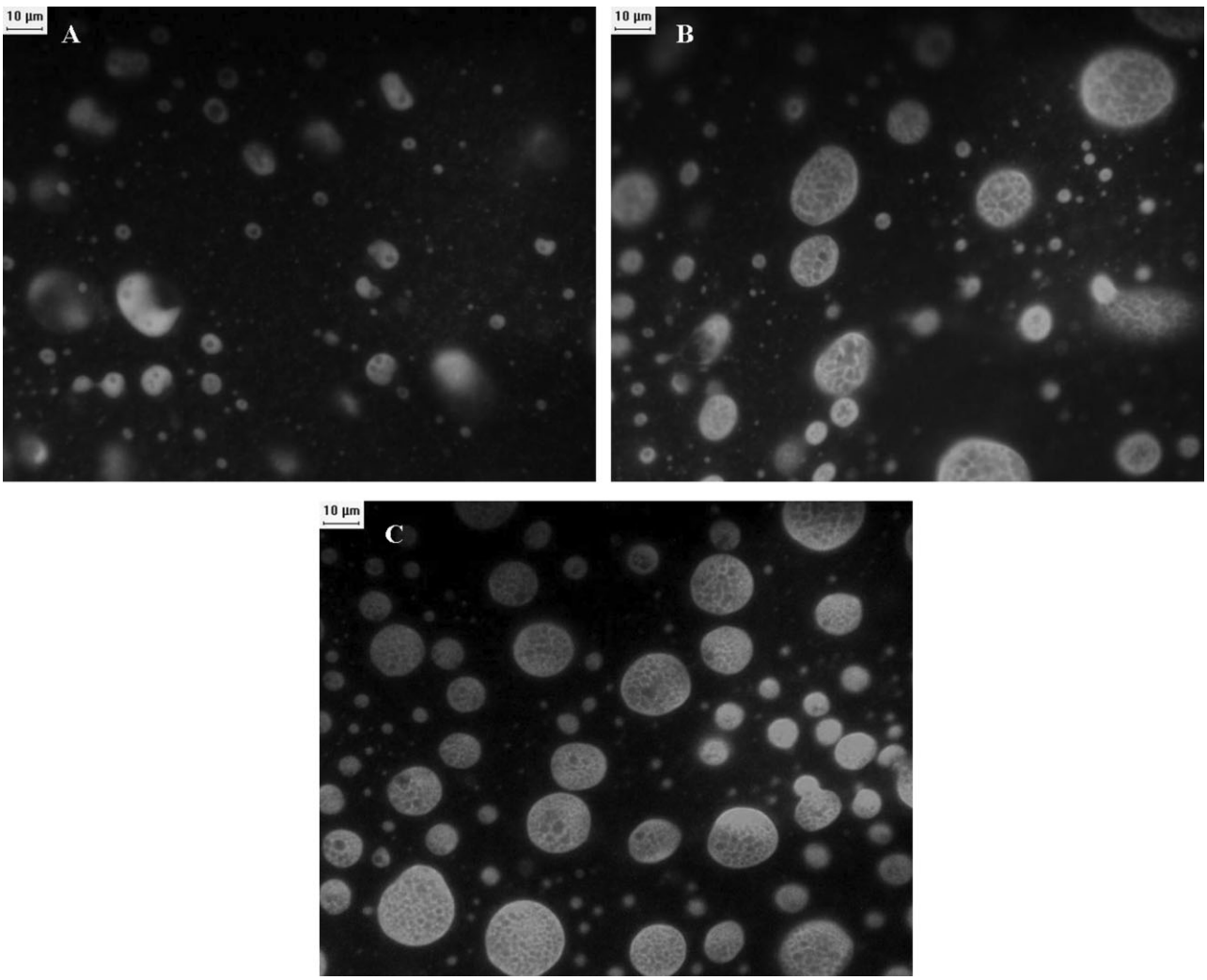

Figure 16 Fluorescence micrographs of samples A, B, and C, respectively.

CONCLUSIONS

The FPMA treated here show that chemical modification of a tapered block styrene-butadiene copolymer before blending with asphalt leads to compatibilized PMA with rheological behavior corresponding to those with weak networks. The larger effects on rheology of asphalt due to the polymer addition were observed in sample C, which possesses five epoxy groups per polymer chain. The increase of the degree of modification of the polymer with epoxy groups leads to increasing viscoelastic properties of the PMA even when functionalization of copolymer is small.

The FPMA displayed high stability at storage temperatures (180°C). At low temperatures, creep data were predicted by simple viscoelastic models, which enabled the analysis of the elastic response of the systems at short times (elastic compliance) and the viscous behavior at long times. Sample B showed the largest activation energy for viscous deformation, which is in turn related to the high resistance to irreversible deformations under strain cycles. From these analyses it was possible to evaluate the FPMA and establish guidelines for the suitability of these materials.

At moderate and high temperatures, the sample B was envisioned as a viscoelastic emulsion, as confirmed by the predictions of the complex modulus versus temperature with an emulsion model. The hard/soft relaxation and droplet relaxation time scales and temperatures were determined for sample B. The slope of the loss modulus in the low-frequency range of the spectrum displays a value close to 0.7, which is larger than that found in the SBS block copolymers (0.5). This indicates that the modification of the relaxation spectrum in FPMA due to the existence of a network is not as strong as in normal PMA. Therefore, a weak network is formed in the case of sample B, and becomes stronger as the degree of epoxy-modification of the rubber is

increased. This is verified in the micrographs that show the morphological features of each FPMA treated here.

REFERENCES

1. Lewandowsky, L. H. Rubber Chem Technol 1994, 67, 447.
2. Adedeji, A.; Grunfelder, T.; Bates, F. S.; Macosko, C. W. Polym Eng Sci 1996, 36, 1707.
3. Brûlé, B.; Brion, Y.; Tanguy, A. Asphalt Paving Technol 1988, 57, 41.
4. Nadkami, V. M.; Shendy, A. V.; Mathew, J. Ind Eng Prod Res Div 1985, 24, 478.
5. Wen, G.; Zhang, Y.; Sun, K.; Fan, Y. Polym Test 2002, 21, 295.
6. King, G.; King, H.; Brûlé, B. Rubber Chem Technol 1990, 63, 637.
7. Christensen, D. W.; Anderson, D. W. Asphalt Paving Technol 1992, 61, 67.
8. Bouldin, M. G.; Collins, J. H.; Berker, A. Rubber Chem Technol 1991, 64, 577.
9. Gahvari, F. J Mat Civil Eng 9, 1997, 111.
10. Wang, Q.; Liao, M.; Wang, Y.; Ren, Y. J Appl Polym Sci 2007, 103, 8.
11. Ohtsuka, Y.; Oshino, Y.; Tanaka, M. U.S. Pat. 5,840,809 (1998).
12. Shim-Ton, J.; Kennedy, K. A.; Piggott, M. R.; Woodhams, R. T. Rubber Chem Technol 1980, 53, 88.
13. Hicks, R. G.; Finn, F. N.; Monismith, C. L.; Leahy, R. B. Asphalt Paving Technol 1993, 62, 565.
14. Anderson, D. A.; Kennedy, T. W. Asphalt Paving Technol 1992, 61, 67.
15. Brodynyan, J. G.; Anderson, D.; Dickinson, E. J.; Witt, H. P. Trans Soc Rheol 1974, 18, 591.
16. Rosedale, J. H.; Bates, F. S. Macromolecules 1990, 23, 2329.
17. Lesueur, D.; Gerard, J. F.; Claudy, P.; Létoffé, J. M.; Martin, D.; Planche, J. P. J Rheol 1998, 42, 1059.
18. Palierne, J. F. Rheol Acta 1990, 29, 204.
19. Lesueur, D.; Gérard, J. F.; Martin, D.; Planche, J. P. CR Acad Sci Ser IIb: Mech Phys Chim Astron 1997, 325, 615.
20. Graebling, D.; Muller, R.; Palierne, J. F. Macromolecules 1993, 26, 320.